Scientific paper

Synthesis, Characterization, Biological Activities and Ab-initio Study of Transition Metal Complexes of [Methyl 2-((4-chlorophenyl)(hydroxy)methyle) Acrylate]

Shazia Ishfaq,[1] Shazia Nisar,[1,*] Saqib Ali,[2] Sadaf Iqbal,[1] Saima Imad,[3] Samina Iqbal,[3] Saeeda Bano,[3] Syeda Kanwal Zahid,[1] Nasreen Fatima[1] and Muhammad Shahzaman[4]

[1] *Department of Chemistry, Faculty of Sciences, University of Karachi, 75270, Pakistan*

[2] *Department of Chemistry, Faculty of Sciences, University of Kotli, 11100, Pakistan*

[3] *PCSIR Laboratories Complexes, Karachi, 75270, Pakistan*

[4] *School of Atmospheric Sciences, Nanjing University of Information Science and Technology, Nanjing 210044, China*

** Corresponding author: E-mail: shazian@uok.edu.pk*
Phone No.00923343519338

Received: 11-29-2021

Abstract

Taking cognizance of the medicinal significance and diverse functions of synthetic Morita-Baylis-Hillman adducts (MBHA), the title ligand was synthesized and purified through column chromatography. Cr^{+3}, Mn^{+2}, Co^{+3}, Ni^{+2}, Cu^{+2} complexes of the ligand were synthesized under basic conditions, subjected to characterization through spectral analyses and verified with the IR spectrum that was generated computationally by the DFT B3LYP method, with 6-311++ G (d,p) basis set and Hartree Fock (HF) B3LYP method in conjunction with 3-21G(d,p) basis set. Powder XRD helped to testify crystals of the complexes. Moreover, the antibacterial, and antioxidant characteristics of MBHA and its complexes were also established. All of them were found to be active antioxidants. The antibacterial activities, examined against *S. aureus, E. coli, B. pumilis and S. typhi* have revealed that its Cobalt complex has an excellent potential to act against all of them. Hence, these compounds maybe having potentialities for the discovery of new, cheaper and efficient drugs against various infectious diseases. The study also uncovers the first example of utilization of MBHA towards metal complex formation.

Keywords: MBH Adduct; transition Metal Complexes; XRD; antibacterial Activities; antioxidant Activities

1. Introduction

The significance of reactions that proceed through Carbon-Carbon bond forming, which in turn involves the coupling of the α-position of activated alkenes with carbon electrophiles under the influence of a catalyst, cannot be overlooked in atom economy.[1,2] The reaction ends up in the formation of Michael type dimers. There are many other synthetic routes by which effectual and perfect C–C bond emerging reactions take place.[3] Further to that medicinally relevant pharmaceutical compounds and natural products are very useful multifunctional building blocks for C–C bond formation which is vital for the synthetic organic chemistry.[4,5] Besides this, Morita-Baylis-Hillman (MBH) compounds, especially the ones which are carbonate, aldehyde, ester, or acetate-based derivatives act as an important intermediate in the synthesis of different structures. These compounds have become important MBH originators and represent a valuable class of substrates for synthetic purposes. These derivatives are widely employed as intermediates in the preparation of significant classes of compounds, as building blocks for natural products. Moreover, Michael/aldol cyclic reactions, that involve multiple C–C bond formations, also lead to important carbon frames that can be employed in drug synthesis.[6] The MBH reaction is mainly a three-component reaction between the α-position of activated alkenes e.g ethyl or methyl acrylate, acrylonitrile and methyl vinyl ketones and electrophilic sp^2 carbon of aldehyde or imines in the presence of an appropriate catalyst, usually a tertiary

amine or phosphine.[5] The resulting Morita-Baylis-Hillman adducts (MBHA) have diverse functionalities and versatile reactivity. Consequently, they have been widely used as powerful precursors for the building of various carbocyclic, heterocyclic and biologically important compounds.[7] These compounds that are economical and biological friendly, perform a number of functions and most importantly can be synthesized following green- one-step synthetic protocols. The anti-fungal, antimalarial, anti-tubercular activities of some MBHAs have been reported.[8] The antileishmanial/antibacterial activities of some MBHA indicate that they can prove to be a novel and promising class of anti-parasitic compounds.[9,10]

In this scenario a discovery that paved the way for some newer treatments has been that of an uncharted world of metal-based chemotherapeutic agents which have dissimilar kinetic and mechanisms of action from those of traditional organic medications. Curative potentialities of metal complexes in tumor/cancer therapy as well as other biological functions develop certain intricacies because central metals exhibit some special features. These metal-based complexes have variable coordination modes, that generate curing drug activity and provide excellency in terms of reactivity in the realm of the organic substrate.[11,12] Through metal complexation of ligands, comprising of oxygen, nitrogen, hydroxyl, or ester functional groups, with metals like copper, zinc, cobalt, and iron, numerous finely-tuned therapeutic activities such as antihypertensive, antimalarial, and antimicrobial get enhanced. In addition, transition metal ion complexes are known to have a key electron transfer role in many biological processes.[13] Metals have long been used for medicinal purposes in a more or less empirical fashion, in a wide variety of chelating modes, geometrical forms, and redox states. Presently identified thermodynamic and kinetic properties of the metal cation and ligand itself, however, provide the medicinal chemist a wide spectrum of reactive sites that can be highly mobilized.[14] Thus, the biological diversity of the transition metal complexes along with their pharmacological specificity is to be established. Promising physiological responses would be drugs need to be demonstrated by in vitro study with targeted biomolecules and tissues as well as in-vivo. Therefore, studies pertaining to ligands with multiple, medicinally dynamic binding sites may serve as models for ensuring biochemical processes.[11,15,16] In this context, the wide variety of potent biotic activities of MBHA encouraged us to synthesize new series of products belonging to this class of compounds, possessing different functionalities and exhibiting potential antioxidant activity. Keeping in view the significance of reported research on synthetic MBH adducts as medicinally important candidates and having the diversity of functions, we conferred them as ligands for the novel drug synthesis composed of their transition metal complexes. The present study is directed towards synthesis, characterization, and computational studies of halo/chloro-benzaldehyde based MBH adducts and some of their novel metal complexes.

2. Materials and Methods

2. 1. General

In the present study various solvents such as n-hexane, methanol and ethyl acetate of synthetic grade were used. In addition to that chemicals 4-Chlorobenzaldehyde (Sigma Aldrich), DABCO (Sigma Aldrich), Methyl Acrylate (Dae-Jung Kosdaq Reagents and Chemicals), NaCl (Sigma Aldrich), $MgSO_4$ anhydrous (Sigma Aldrich), NaOMe (Dae-Jung Kosdaq Reagents and Chemicals), $CuCl_2 \cdot 2H_2O$ (Sigma Aldrich), $MnCl_2 \cdot 2H_2O$ (Sigma Aldrich), $NiCl_2 \cdot 6H_2O$ (Sigma Aldrich), $CoCl_3 \cdot 6H_2O$ (Sigma Aldrich) and $CrCl_3.6H_2O$ (Sigma Aldrich) were used. Further to that equipments like UV lamp (monitoring TLC card), Digital hot plate with constant temperature and stirring system, Gallen Kamp melting point instrument, LAMBDA 1050+ UV/Vis/NIR spectrophotometer, FTIR Spectrophotometer of Shimadzu Company prestige-21. The ^{1}H NMR spectrum of the ligand was recorded on AVANCE NEO NMR spectrometer (500 MHz for ^{1}H) in $CDCl_3$ solvent. Chemical shifts are reported as δ ppm against TMS as internal reference and coupling constants (*J*) are reported in Hz units. Mass spectrophotometer instrument of JEOL 600H1, for transition metal complexes used Electrospray ionization mass spectrometry (ESI MS) at QTrap hybrid triple-quadrupole (QTrap 2000, Applied Biosystems/MDS Sciex) and XRD Pananalytical company X-pro serial No. DYH313 for powder diffraction were the major instruments used for data analysis.

2. 2. Synthesis of MBHA *(Methyl 2-((4-chlorophenyl) (hydroxy)methyle) acrylate)* L1

MBHA was prepared by addition of 5 equivalents of methyl acrylate to 4-chloro benzaldehyde (1 equivalent). The reaction mixture was further treated with 0.65 equivalents of Lewis base DABCO, using 5% THF solvent in round bottom flask with constant stirring at room temperature. The progress of the reaction was monitored at regular intervals of one hour through TLC under UV lamp and the completion time was recorded as 24 hours. The excess of methyl acrylate was evaporated which furnished gummy crude material upon complete evaporation. This was diluted further with 15 mL each of ethyl acetate and brine solutions. The organic layer developed in this mixture was separated through separating funnel, collected and this process was repeated thrice. Furthermore, the organic phase was concentrated by removing EtOAc through evaporation and concentrated crude was subjected to column chromatographic purification. Mobile phase system of ethyl acetate and n-hexane in ratio of 5:95 to 35:65 (v/v) was used for this

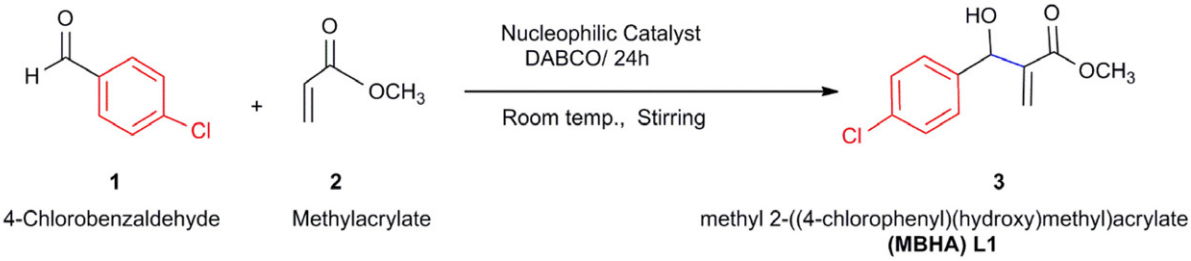

Scheme 1. Morita-Baylise Hillman reaction with e.g. aldehydes by using tertiary amine (DABCO) as catalyst at room temperature and other standard reaction conditions

purpose. The main spot was collected as product in pure form and it's purity was confirmed through spectral analysis.[7,9,17] The experimental ^{1}H NMR and mass spectrum is in good agreement with previous studies[18,19] and hence proves the purity of the final MBHA synthesized using this procedure. Preparation of the MBHA is shown below in scheme 1.

A pearl white color gummy mass was found in the form of pure product of $C_{11}H_{11}ClO_3$ (compound **3**) yield 80% (226.66 g/mol). B.P: 125.3–125.5 °C. IR data (KBr: νmax, cm^{-1}): 3446, 2953, 2897, 1714, 1631, 1487, 1440, 1278, 1151, 1045,827 and 540. ^{1}H NMR (500 MHz, $CDCl_3$): δ 3.29 (s, 1H, OH), 3.71 (s, 3H, OCH_3), 5.55 (m, 2H, CH_2), 5.83 (s, 1H, CH), 6.35 (s, 1H, H-1), 7.49 (d, $J_{2,3}$ =8 Hz, H-2, H-3, Ar), 7.60 (d, $J_{5,6}$ =6.5 Hz, $J_{5,1}$ = 1.5 Hz, H-4, H-5, Ar), ppm. UV-visible data in DMSO [λ, nm (ε, M^{-1} cm^{-1})]: 267(124.23). [(m/z) M$^+$, Cal./Obs. (%)] for $C_{11}H_{11}ClO_3$: 227 (56) M$^+$, 207 (25), 191 (100), 160 (90), 132 (66), 104 (70), 77 (64).

2. 3. Synthesis of Metal Complexes with Ligand MBHA (L1)

About 20 mL of 0.02M each metal salt solutions in distilled water and 0.04M solution of L1 in hot ethanol were prepared separately (1:2). The metal salt solution was added with continued stirring to adduct solution drop wise, few drops of NaOH were added to maintain the pH at 11. The reaction mixture was refluxed at 60–70 °C with constant stirring for 3–5 hours until solid mass formed in the mixture.[15,20] Only one spot appeared for the desired molecule on TLC strip suggesting its purity. After completion of the reaction (complete solid mass formation), the reaction mixture flask was cooled slowly at room temperature and precipitates were collected using vacuum filtration. The precipitates were washed thrice with ethanol and distilled water. Then the obtained product was dried in a desiccator. The deduced structural formula for each of the transition metal complex is shown in scheme 2.

2. 4. Analytical Data of Transition Metal Complexes

CrL1 complex (compound **4**) 577.37(g/mol), Light blue: m.p: >300 °C. IR data (KBr: νmax, cm^{-1}): 3500–3380, 2915, 2980, 1708, 1625, 1550, 1438, 1382, 1105, 835, 603 and 520. UV-visible data in DMSO [λ, nm (ε, M^{-1} cm^{-1})]: 262(145.9). [(m/z) M$^+$, Cal./Obs.(%)] for $C_{22}H_{30}Cl_2O_{10}Cr^{3+}$: 192.02(100)/192.69(65.1)M$^+$.

CoL1 complex (compound **5**) 584.31(g/mol), Dark brown: m.p: >300 °C. IR data (KBr: νmax, cm^{-1}): 3500–3400, 2935, 1651, 1620, 1483, 1386, 1109, 837, 653, 607 and 518. UV-visible data in DMSO [λ, nm (ε, M^{-1} cm^{-1})]: 260(136.58). [(m/z) M$^+$, Cal./Obs.(%)] for $C_{22}H_{30}Cl_2O_{10}Co^{3+}$:194.35(100)/195.02(63.9) M$^+$.

NiL1 complex (compound **6**) 548.04 (g/mol), Parrot green: m.p: >300 °C. IR data (KBr: νmax, cm^{-1}): 3450–3350, 3005, 2850, 1640–1566, 1643, 1566, 1463, 1388, 1109, 609 and 455. UV-visible data in DMSO [λ, nm (ε, M^{-1} cm^{-1})]: 255(139.54). [(m/z) M$^+$, Cal./Obs.(%)] for $C_{22}H_{26}Cl_2O_8Ni^{2+}$: 274.01(100)/273.02(97.6)M$^+$.

MnL1 complex (compound **7**) 544.28(g/mol), Blackish brown: m.p: >300 °C. IR data (KBr: νmax, cm^{-1}): 3505–3310, 3005, 2980, 1629, 1500, 1566, 1386, 1111, 748, 603 and 523. UV-visible data in DMSO [λ, nm (ε, M^{-1} cm^{-1})]: 253(128.10). [(m/z) M$^+$, Cal./Obs.(%)] for $C_{22}H_{26}Cl_2O_8Mn^{2+}$: 271.52(100)/272.52(65.6)M$^+$.

CuL1 complex (compound **8**) 552.89 (g/mol), Paris green: m.p: >300 °C. IR data (KBr: νmax, cm^{-1}): 3480–3350, 3115, 2980, 1673, 1604, 1521, 1388, 1112, 746, 605 and 486. UV-visible data in DMSO [λ, nm (ε, M^{-1} cm^{-1})]: 250(161.10). [(m/z) M$^+$, Cal./Obs.(%)] for $C_{22}H_{26}Cl_2O_8Cu^{2+}$: 276.51(100) /275.51 (89.5)M$^+$.

2. 5. Computational Studies

All the calculations were performed with the Gaussian 16W [21] program package on a ACPI x64 Core i7 laptop with 3.0 GHz processor and 16 GB Ram. The molecular structure of ligand in the ground state is optimized by using DFT B3LYP method and 6-311++ G (d,p) basis set.[23,24] The molecular structures of remaining metal complexes are optimized by UFF molecular mechanics. The vibrational frequencies of ligand and nickel metal complex were also calculated along with optimization. The assignment of the calculated wavenumbers is aided by the animation option of Gauss View 6.0 graphical interface for Gaussian program, which gives a visual presentation of the shape of the vibrational modes.

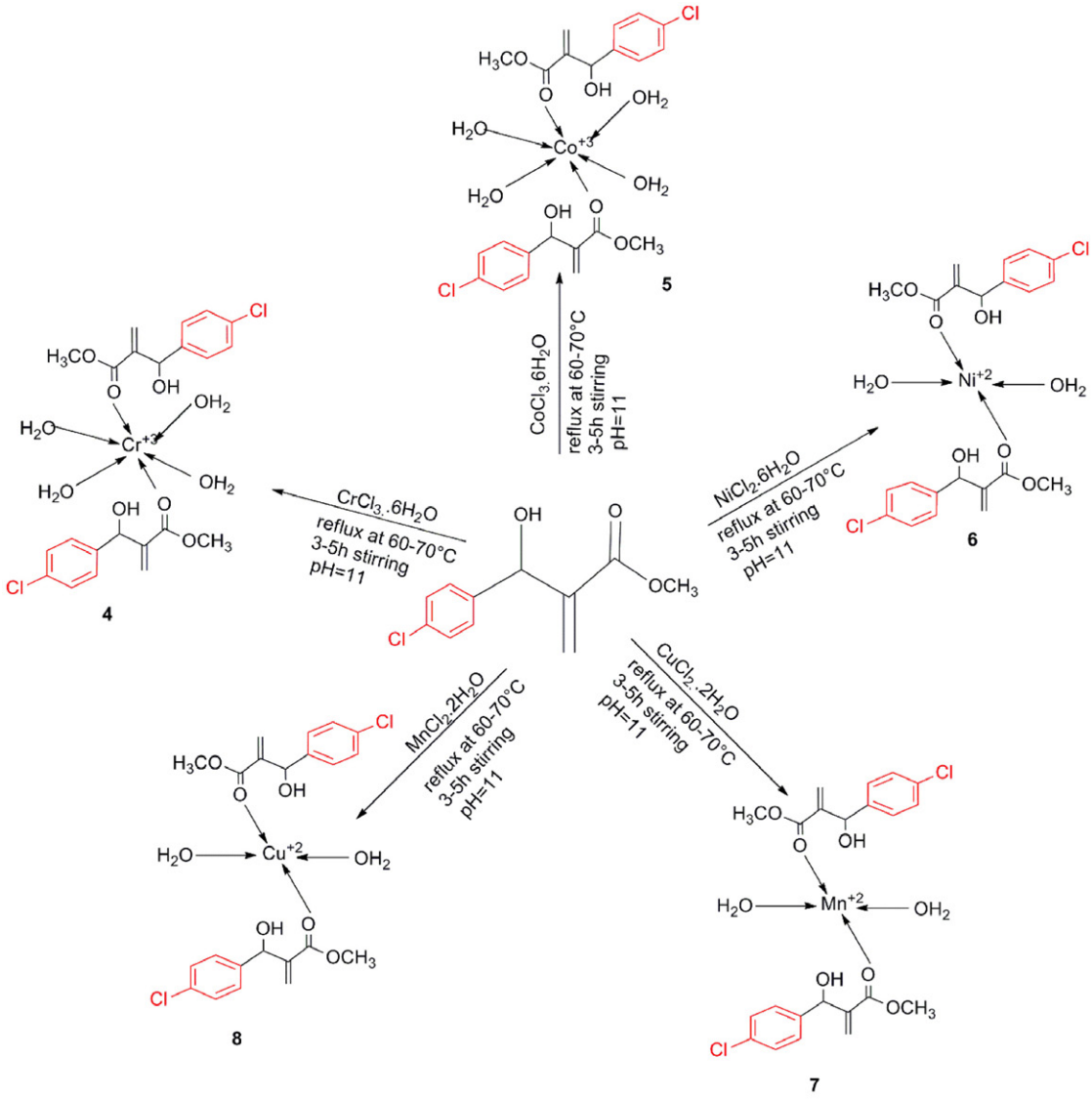

Scheme 2. Molecular modifications by reacting the MBHA as Ligand with transition metal salts to synthesize corresponding metal complexes

2. 6. X-Ray Diffraction

The XRD study (powder pattern) of the complexes were made with the help of X-ray diffractometer (Goniometer Radius mm = 240.00 and Dist. Focus-Diverg. Slit mm = 91.00) with Cu- anode material, Kα [A˚] = 1.54060 and the generator settings 30 mA, 40 kV.

2. 7. Antibacterial Assay

The antibacterial activity of L1 and its complexes was evaluated by agar diffusion method,[26,27] against two Gram-negative bacteria (*Staphylococcus aureus, Escherichia coli*) and two Gram- positive bacteria (*Bacillus pumilis, Salmonella typhi*). All extracts were sterilized by sterile membrane syringe filter (pore size 0.45µm, Millipore). For assay, 1mL of culture suspension of each strain (25% transmittance, 530 nm) was added in 100 mL antibiotic agar No.11 (45 °C) and mixed well. 25mL of inoculated agar was poured in each petri dish (20 × 100 mm) and kept for solidification. After solidification 4 holes were made using sterile borer of 8mm diameter with 6mm internal diameter. Holes were marked and each extract (100 µL) was poured in the respective well, and incubated for 24 hours at 37 °C. The experiment was performed in triplicate under strict aseptic conditions. After incubation, zone of inhibition (mm) produced by each extract was measured and antibacterial activity expressed in terms of percent inhibition. Gentamycin (0.3%) was used as a standard antibiotic in comparison to L1 and complexes.

2. 8. DPPH Radical Scavenging Activity

The free radical scavenging action was determined by using the DPPH (2,2-diphenyl-1-picrylhydrazyl) radi-

cal scavenging method with some modification.[28,29] The 0.3 mM solution of DPPH was prepared in methanol. 10 µL of each sample of different concentration (25 µg–100 µg) was mixed with 1.0 mL of DPPH solution. The reaction mixture was incubated at 37 °C for about 30 min. The absorbance at 515 nm was measured by spectrophotometer and percent radical scavenging activity was determined in comparison with the methanol treated control. Ascorbic acid was used as standard for further samples analysis.[30] By using this standard the antioxidant activity of the MBHA (L1) and its metal complexes were determined and recorded in the Table 4.

3. Results and Discussions

The present work was initiated with (i) the synthesis of ligand MBHA ($C_{11}H_{11}ClO_3$) through MBH reaction scheme where the choice of catalyst in appropriate amount and solvent often have a significant effect on the efficiency, rate and stability of the reactions.[31,32] Using DABCO as catalyst and THF as solvent, the MBH adducts form exclusively or as major products in moderate to good yields in stable form upon continues stirring.[33,34] The stability of the adduct was further confirmed via spectral analysis, which demonstrated no dimerization (Scheme 1), its transition metal complexes with five biologically significant transition metal ions

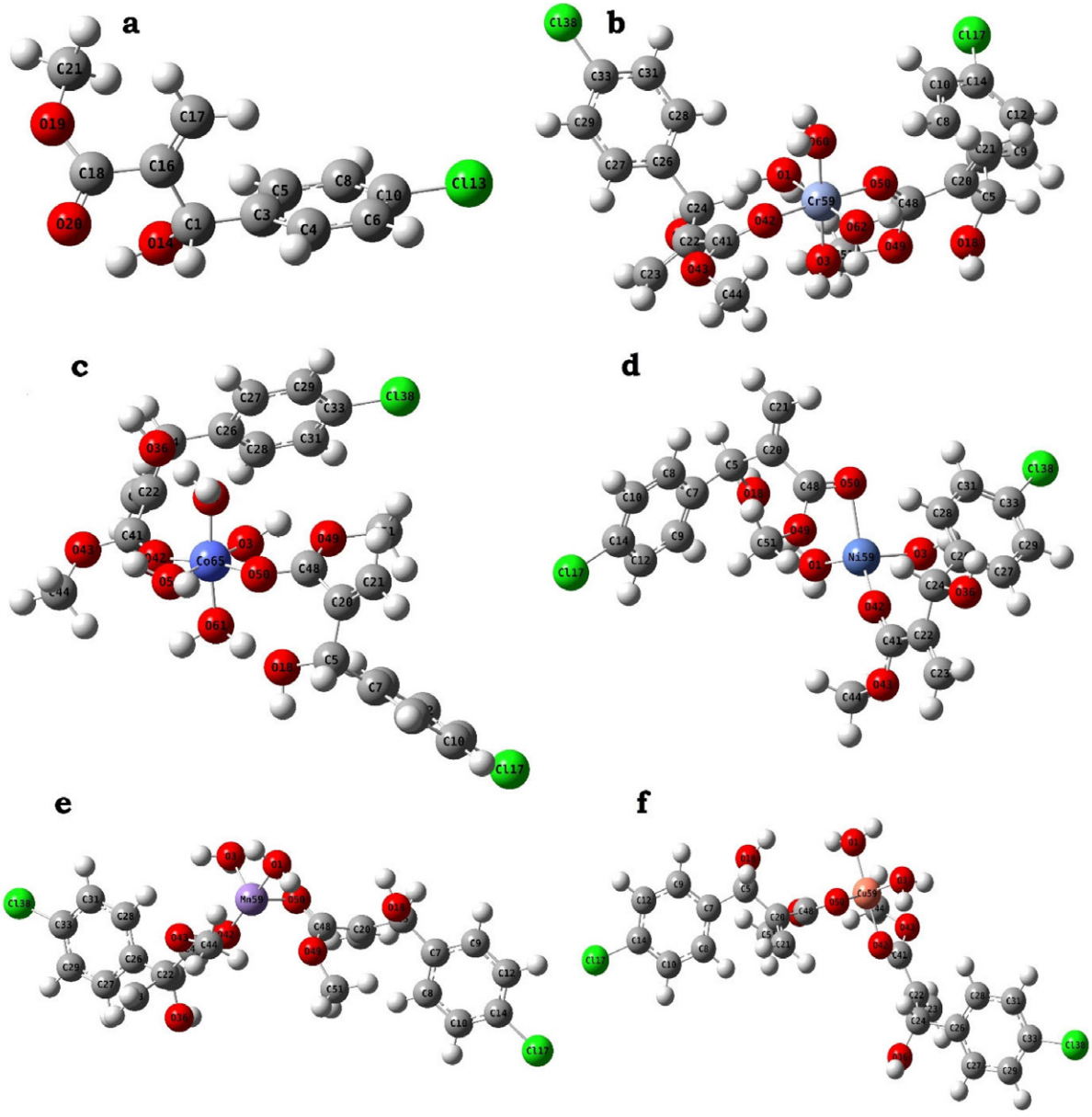

Fig. 1. Theoretically optimized geometry of the (a) MBHA (L1), and its corresponding complexes, (b) $Cr^{+3}L1$, (c) $Co^{+3}L1$, (d) $Ni^{+2}L1$, (e) $Mn^{+2}L1$ and (f) $Cu^{+2}L1$. The results have confirmed that each metal is coordinated by two ligand molecules, Cr^{+3}, Co^{+3} are octahedral and Ni^{+2}, Mn^{+2}, Cu^{+2} are tetrahedral as per optimized geometrical structures.

(Scheme 2), (ii) characterization of these compounds and finally (iii) their subsequent biological and antioxidant investigations. The UV-Visible spectroscopic results have revealed the formation of metal complexes, which was observed between 250 nm–265 nm of wavelength, in contrast to MBHA (L1) that shows a λ_{max} = 267 nm. Additionally, the m/z ratio and relative abundance (%) of MBHA have also been observed using Electrospray ionization-mass spectrometry (ESI-MS). [35]While, the ^{1}H NMR of MBHA was recorded at 500MHz using $CDCl_3$ as solvent. MBHA (compound **3**) showed four signals at δ 3.29, 3.71, 5.83 and 6.34 ppm as singlet corresponding to proton of –OH and three proton of $–OCH_3$, one proton of –CH and one –CH aromatic proton, respectively, in ^{1}H NMR spectrum. Furthermore, one signal of multiplet was appeared at δ 5.55 because of two protons of $–CH_2$ and neighboring proton effect. The other aromatic protons have been shown in the region δ 7.47–7.49 and 7.60–7.62 as doublet ppm in consensus with the structure.[36–38] In Mass spectrum,[8] a prominent peak of 227 m/z at 56.5% noted for $M^{+,}$ while 207 m/z (25%), 191 m/z (100%), 160 m/z (90%), 132 m/z (66%), 104 m/z (70%) and 77 m/z (64%) for fragmentation peaks pertaining to synthesized MBHA were recorded. The ^{1}H NMR and ESI-MS spectral data are consistent with the assigned structure (compound **3**). Additionally, the results of computational and spectral studies confirm that each transition metal (Cr^{+3}, Co^{+3}, Ni^{+2}, Mn^{+2}, Cu^{+2}) complex with MBHA (L1) has 1:2 stoichiometric ratios (Fig. 1).

3. 1. Theoretical and Experimental FTIR Analysis of Ligand (MBHA)/Compound 3

The FTIR spectra of MBHA (L1) and their complexes $[M(L1)_2(H_2O)_4]^{+3}$, $[M(L1)_2(H_2O)_2]^{+2}$ were recorded between 4000–500 cm^{-1} using KBr disk and the data is presented in Table-2. The FTIR data corresponding to compound **3**, has shown the characteristics -OH broad peak in 3446 cm^{-1}, prominent stretch of =C-H at 2953 cm^{-1} and Sp^3 C-H stretch at 2897cm^{-1}. The band observed at 1714 cm^{-1} is due to ester carbonyl vibration. Furthermore, the frequency ($\bar{\nu}$) of C=C aromatic, $-CH_3$, C-O and C-Cl were designated as 1631 $cm^{-1,}$ 1440 $cm^{-1,}$ 1278cm^{-1} and 540 cm^{-1} respectively (Fig. 2a).[39] Moreover, in computational IR analysis, it was observed that OH peak is somewhat different from the observed spectrum. This fact is because of the breadth of OH band appeared by the water vapors. It might be obtained due to greater number of OH ions appeared in the same intensity.[40] The peak intensities

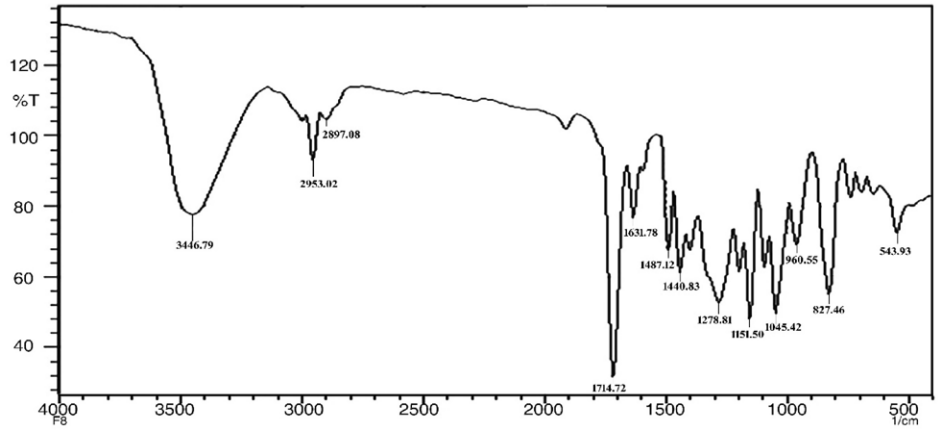

Fig. 2a. Experimental FTIR spectrum of Methyl 2-((4-chlorophenyl)(hydroxy)methyle) acrylate [MBHA (L1)]

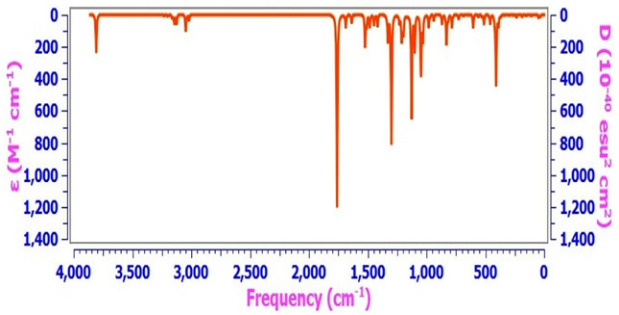

Fig. 2b. Theoretical FTIR spectrum of Methyl 2-((4-chlorophenyl)(hydroxy)methyle) acrylate [MBHA (L1)]

of left aforementioned fragments (Fig. 2b) in calculated spectrum more about the similar values. The slight change may be observed because of the theoretical results presented to isolated functional groups in gaseous state, while the experimental calculations belong to the molecules in solid state.[41]

3. 2. Characterization of MBHA Based Metal Complexes

The transition metals (Cr^{+3}, Co^{+3}, Ni^{+2}, Mn^{+2}, Cu^{+2}) complexes of MBHA (L1) were synthesized. Initially, Cr^{+3}

based complex **4** of ligand was prepared by employing a reported method.[42] The existence of a single complex specie in the reaction mixture and hence, the purity of the complex was confirmed through TLC, until a single spot was achieved on TLC plate (expected product **4**) (Scheme 2). In addition to this, the major spot upon purification was subjected to UV- visible analysis, which presented considerable difference from MBHA band (expected product **4**). By repeating the procedure with slight modification such as increasing the pH, precipitates were observed in 2.5 hours. Furthermore, the TLC analysis indicated 20–30 percent conversion with less spots and change in color. Based on current observation (TLC in 1.5h), any increase in the concentration of base up to 4M, maximum conversion of the reactants into product was observed (Scheme 2).

All the transition metal complexes (**4-8**) were subjected to characterization through their physical characteristics. Their molecular and structural formulae were established with the help of m/z ratio obtained through powder XRD and FTIR analyses. The data presented for m/z ratio of the ligand and compound **4-8** shows a good agreement between the calculated and observed values and thus support the suggested structures of the complexes.

3. 3. Theoretical and Experimental FTIR Analysis of the Compounds 4-8

Table 1 provides the details of the experimental and computed IR vibrational frequencies of MBHA (compound **3**) and metal complexes (compounds **4-8**). Considering FTIR spectrum of compound **4**, a broad band at 3500–3380 cm^{-1} (–OH) can be observed, which might be either due to moisture or coordinated water in the complex. Moreover, we observed peak shifts toward lower frequency value for C=O group from a sharp peak of ligand at 1725 cm^{-1} to a small peak at 1625 cm^{-1}. It suggests the coordination of carbonyl group through oxygen to the Cr^{+3} metal which ultimately reduces strength of the carbonyl group in complex. These results are also supported by literature.[14] Similarly, the peaks of ligand and its C-O (of ester) appeared 1278 cm^{-1} which showed a shift from 1105 cm^{-1} (Table 1). Which may change because of environmental effect regarding C=O coordination towards the metal ion.[43,44] Some additional peaks have also been observed to appear at 603 and 520 cm^{-1}. These peaks were assigned to Cr-O and C-Cl, respectively.[45] These findings have confirmed the participation of carbonylic functional group of the ligand in complex formation. No significant change in the IR frequency of C=C double bond was seen upon complex formation and hence, it is inferred that this group doesn't participate in complexation (Fig. 1b). Based on these observations, the molecular and structural formulae of the compound **4** were deduced as $[Cr(L1)_2(H_2O)_4]^{+3}$.

In FTIR spectral results for the compound **5** we observed that –OH group has shown a broad signal ranging from 3400–3300 cm^{-1}. This signal was relatively at similar position as in the ligand. While comparing the C=C frequencies of both the ligand and complex **5**, the peak was found to be slightly shifted from 1631 cm^{-1} to 1620 cm^{-1} which suggests that this functional group was not involved in coordination. The aromatic ring has shown frequencies (1604 and 1521cm^{-1}) almost at similar position as that of the ligand aromatic pi bonds which also suggests non coordination behavior of the aromatic ring in respective complex formation. A clearer signal appeared at 1651 cm^{-1} was probably due to the carbonyl group and has significantly shifted from 1714 cm^{-1} to 1651 cm^{-1} upon complexation. This kind of shift has also been reported in literature,[14] thus confirming the coordination of the ligand's carbonyl site to the Co^{+3} metal. Another significant variation in the IR spectrum of complex was a slight shift to the higher frequencies in IR signal of C-O (of ester) i.e. ligand C-O frequency shifted from 1278 to 1386 (C-O of the complex) (Table 1). Additionally, a unique signal attributable to Co-O appeared at 607 cm^{-1} and another noticeable

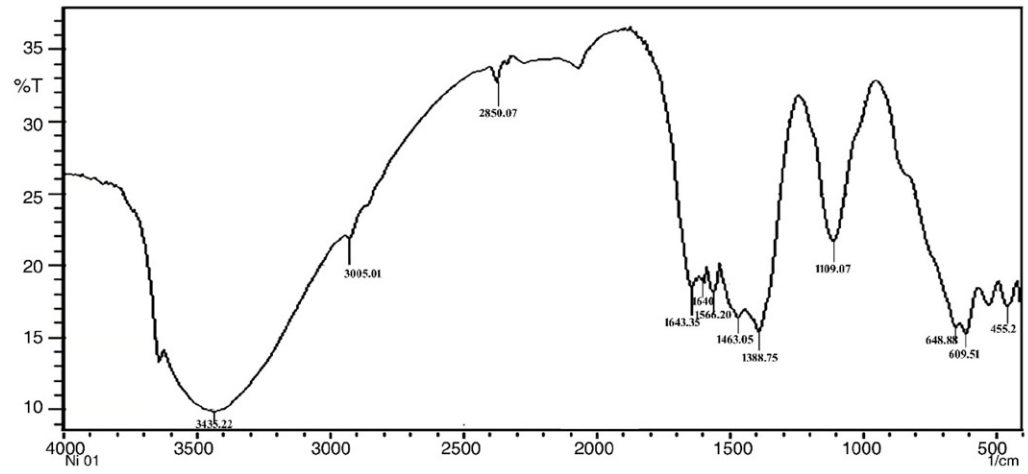

Fig. 3a. Observed FT-IR spectrum of Nickel Transition Metal with MBHA (L1)

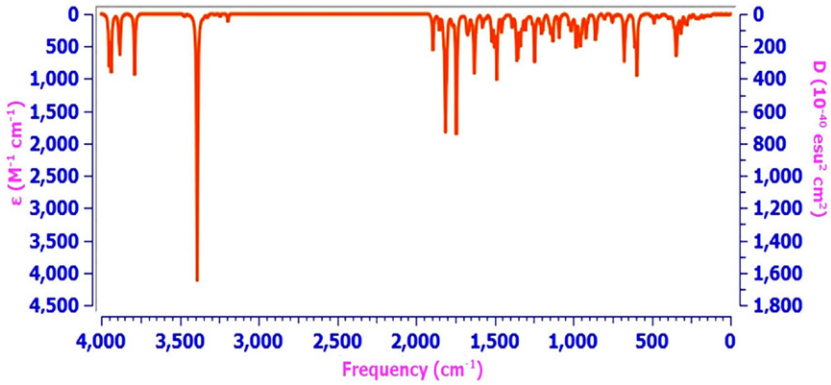

Fig. 3b. Theoretical FT-IR spectrum of Nickel Transition Metal with MBHA (L1)

variation in C-Cl frequency from 540 cm^{-1} to 518 cm^{-1} was also observed. Based on the overall information discussed above, the molecular formula $[Co(L1)_2(H_2O)_4]^{+3}$ and structural formula (Fig. 1c) was established for the compound **5**.

FTIR analysis for the Ni^{+2} complex (compound **6**) showed peaks for all the prominent functional groups along with some informative shifts which revealed the complex formation. Such as, an extremely weak band, almost negligible at 1640 cm^{-1} correspond to carbonyl group which was comparatively at lower frequency than its precursor (Ligand) carbonyl absorption (1714 cm^{-1}). It suggests carbonyl coordination upon complex formation. Moreover, the peaks at 609 cm^{-1} and 455 cm^{-1} were assigned to Ni-O and C-Cl groups, respectively. Additionally the –OH and =CH groups exhibited peaks at 3450–3350 cm^{-1} (broad) and 3005 cm^{-1}, respectively. Furthermore, we have also observed peaks for C=C bond at 1643 cm^{-1} with no significant shift and simultaneously demonstrating that C=C do not participate in complexation (Fig. 1d). In spite of that we have also observed sharp peak instead at 3880–3886 cm^{-1} of same (-OH) functional group. The difference is observed due to the presence of moisture in the compound, which has provided interference during recording of spectrum.[41] Likewise, the remaining functional groups show a little change in the calculated values as is evident from their sharp pointed peaks at exact frequencies. In the observed spectrum these small peaks overlap with each other to give loops instead of sharp pointed peaks obtained in the theoretical spectrum (Fig. 3a & Fig. 3b).[40] Nevertheless, we have obtained good agreement in the observed and calculated values of frequencies and deduced the formula $[Ni(L1)_2(H_2O)_2]^{+2}$.[46]

FTIR spectral results for the compound **7** (Fig. 1e) reveal that –OH group gives a broad band ranging from 3505–3310 cm^{-1} with relatively no change in its position as compared to the ligand. Similarly, the C=C $\bar{\nu}$ (1631 cm^{-1}) remains about the same upon complex formation i.e. at 1629 cm^{-1} suggesting that this functional group was not involved in coordination. A clear disappearance of signal of the carbonyl group and its appearance at an entirely new position (Table 1) was probably due to its coordination with the metal ion. This kind of shift has also been reported in the literature,[14] hence confirms the coordination of the ligand's carbonyl site to the Mn^{+2} metal ion. Moreover, the appearance of new peak at 603 $cm^{-1}$was attributed to Mn-O while C-Cl 540 cm^{-1} shifted towards 523 cm^{-1}. The

Table 1. Characteristic FTIR bands of the MBHA (L1) and its metal complexes (cm^{-1}) $\bar{\nu}$

Functional groups	(L1)	Calc. (L1)	CrL1	CoL1	NiL1	Calc. NiL1	MnL1	CuL1
$\bar{\nu}$ **(-OH)**	3446	3808	3500–3380	3300–3400	3350–3450	3880–3886	3310–3505	3350–3480
$\bar{\nu}$ **(=C-H)**	2953	3150	2915	2950	3005	3194	3005	3115
$\bar{\nu}$ **(Sp^3 C-H stretch),**	2897	3020	2810–2980	2860–2935	2850	3244	2980	2980
$\bar{\nu}$ **(ester C=O),**	1714	1760	1625	1651	1640	1669	–	–
$\bar{\nu}$ **C=C (aromatic),**	1631	1637	1550	1620	1643	1627	1629	1673
$\bar{\nu}$ **C=C**	–	1446	1438	1483	1566	1576	1500	1604
$\bar{\nu}$ **($-CH_3$)**	1440	1482	–	–	1463	1485	1566	1521
$\bar{\nu}$ **(C-O)**	1278	1299	1105	1386	1388	1358	1386	1388
$\bar{\nu}$ **(C-OCH_3)**	–	1212	1382	1109	1109	1128	1111	1112
$\bar{\nu}$ **(M-O)**	–	–	603	607	609	606	603	605
$\bar{\nu}$ **(C-Cl)**	540	459	520	518	455	485	523	486

Only the observed changes in specified functional groups are represented

molecular $[Mn(L1)_2(H_2O)_2]^{+2}$ and structural formula were established for the compound **7**.

FTIR results for the compound **8** (Fig. 1f) have revealed the presence of –OH functional group by a peak almost at similar position (3480–3350 cm^{-1}) as that of the ligand precursor. Almost similar results were obtained for the presence of sp^2 and sp^3 C-H bonds of the complex i.e. their peaks were observed at 3115, 2980 cm^{-1} respectively. The ester carbonyl absorption (1705 cm^{-1}) has completely disappeared as compared to that of the ligand carbonyl (1714 cm^{-1}) which suggests its participation in complex formation. No marked difference was observed in the frequency due to the C=C double bond (1673 cm^{-1}) and aromatic C=C bond (1604 cm^{-1}) suggesting no contribution in complex formation. These assumptions were further supported by appearance of IR peaks at 605 cm^{-1}, and 486 cm^{-1} due to presence of Cu-O and C-Cl bond. Based on all these physical, analytical and spectral results the prepared complex was assigned the structure presented above in scheme 2 as compound **8** formulated as $[Cu(L1)_2(H_2O)_2]^{+2}$.

3. 4. X-Ray Diffraction

The structure resolved from powder XRD analysis is a successful process that leads to evaluation of an exact crystal structure depending on the cautious handling of each step. Microcrystalline materials mainly organic based metal complexes can easily be resolved by XRD powder diffraction.[13,28] The accuracy of a material whose structure is to be determined depends on the quality of the powder diffraction data. Besides, nature of the asymmetric unit such as the number, type of atoms, atomic arrangement and molecular geometry involves to prove the quality of the complex. However, for successful structure determination, monophasic powder sample of good crystallinity should be available for the material of interest.[47] The recorded result was summarized in Table 2. & Table 3.

X-ray diffraction was performed for further confirmation of the structure of transition metal complexes. The patterns of diffractograms obtained for complexes are given in Fig. 4. Each metal complex pattern has one sharp peak of metal oxide (Fig. 4). This clearly gives an idea of the coordination of one oxygen atom from the ligand to the metal ions. Hence, the idea of coordination of ligand with the metal ions through the same site has been confirmed. Moreover, these patterns indicate crystalline nature of all the complexes. It can be observed that the rest of the pattern of metal complexes is almost dissimilar from each other owing to the formation of a distinct distorted crystalline structure. Most probably, this difference is due to the coordination of water molecules into the coordination sphere.[15,16] Besides, they have different unit cell number and radius intensity ratio, because of this they belong to non-identical but unique crystal class. The resultant XRD output such as density, volume, radius intensity ratio, lattice parameters (a, b, c, α, β, γ) and probable crystal class have been given in the Table 2. The chromium complex (compound **4**) was isolated, and crystallized in the orthorhombic system (space group Pmmn (59) with Z = 2). In the cobalt complex, the molecule contains one Cr^{+3} atom, two

Table 2. Crystallographic data and observed refinement parameters for complexes **4-8**

S. No.	Sample complexes	S. Group (G. No.)	Volume (10^6pm^3)	Density (g/cm)	Unit Cell Dimensions (Å)	Crystal Class	No. of unit cells (Z)	Reference Intensity Ratio (RIR)
1	**CrL1**	Pmmn (59)	94.58	3.63	**a≠b≠c** a = 3.8630 b = 3.1820 c = 7.6940	Orthorhombic	2	4.60
2	**CoL1**	Fd-3m (223)	93.82	6.09	**a=b=c** a = 8.0840 b = 8.0840 c = 8.0840	Cubic	2	6.39
3	**NiL1**	R-3m (166)	99.78	4.53	**a=b≠c** a = 2.8353 b = 2.8353 c = 14.3319	Hexagonal	3	6.38
4	**MnL1**	141/amd (141)	518.94	…….	**a=b=c** a = 8.0360 b = 8.0360 c = 8.0360	Cubic	4	4.21
5	**CuL1**	Cc (9)	81.12	6.51	**a≠b≠c** a = .6890 b = 3.4200 c = 5.1300	Monoclinic	4	3.72

Table 3. Crystal lattice Data and Summary of Data Collection and Refinement for complexes **4-8**

S.NO.	Complex Compound	Miller Indices			d [Å]	2θ	Intensity (%)
		h	k	l			
1	$[Cr(L1)_2(H_2O)_4]^{+3}$	0	0	1	7.6940	11.492	100.0
		1	0	1	3.4523	25.785	48.3
		1	1	0	2.4519	36.620	37.2
		1	1	1	2.3397	38.443	14.1
2	$[Co(L1)_2(H_2O)_4]^{+3}$	2	2	0	2.8600	31.249	40.0
		3	1	1	2.4380	36.837	100.0
		5	1	1	1.5559	59.350	35.0
		4	4	0	11.4293	65.222	45.0
3	$[Ni(L1)_2(H_2O)_2]^{+2}$	1	1	0	4.7773	18.558	100.0
		1	0	1	2.4201	37.119	26.9
		1	0	4	2.0254	44.706	36.9
		1	0	7	1.5724	58.663	9.4
4	$[Mn(L1)_2(H_2O)_2]^{+2}$	2	1	1	3.4037	26.160	100.0
		1	0	3	2.9359	30.421	20.8
		2	2	0	2.8850	30.972	22.1
		2	2	4	1.8266	49.883	30.9
5	$[Cu(L1)_2(H_2O)_2]^{+2}$	0	2	2	2.5300	35.452	100.0
		2	0	2	2.3600	38.100	79.7
		0	0	4	2.3350	38.525	36.2
		2	2	0	2.0241	44.735	42.2

Each set of indices was chosen on the basis of highest intensity (%) of sharp peak

coordinated MBHA (L1) molecules at the two sites in a mononuclear complex.

It is noteworthy that the complexes cobalt and manganese (compound **5** and **7**) were found to have cubic crystalline nature, having space group Fd-3m (223) and 141/amd (141), whereas they have 2 and 4, Z values, respectively. The indexing related to their structure elucidation as well as peak intensities and diffraction angle (2θ) is given in the Table 3. It is illustrated that the prepared complex of nickel (compound **6**) has the space group R-3m (166), Z =

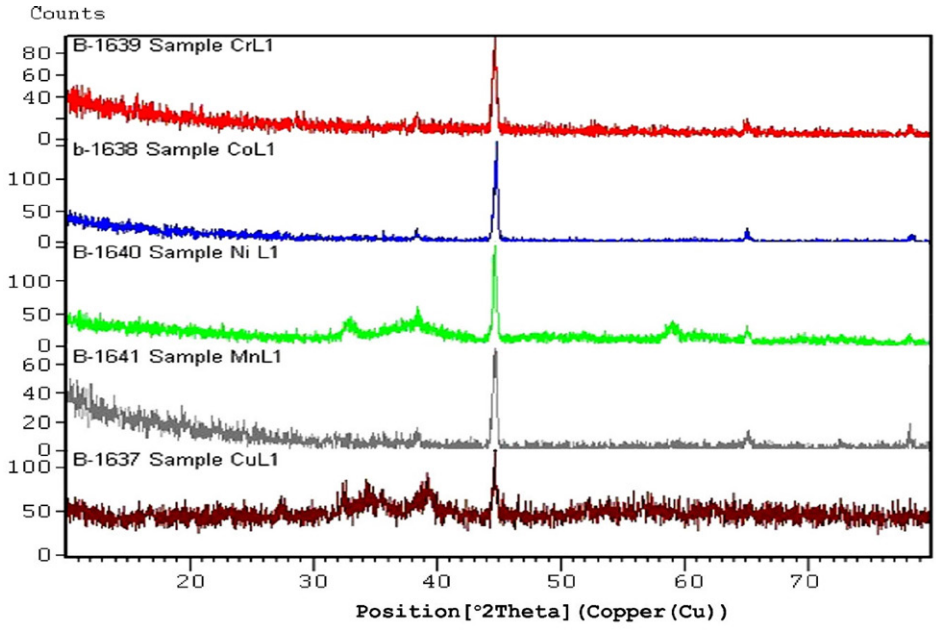

Fig. 4. X-ray diffraction patterns of complexes $[M(L1)_2(H_2O)_4]^{+3}$ with M=Cr^{+3}, $Co^{+3}$and $[M(L1)_2(H_2O)_2]^{+2}$ with M= Ni^{2+}, Mn^{+2} and Cu^{2+}

3 and belongs to hexagonal crystal class. While, copper metal (compound **8**) coordinated with MBHA has monoclinic crystalline nature. It has the space group Cc (9) and Z = 4. Based on aforementioned analysis and to provide more strength in verdicts (energy balance and mass balance) the computational modeling was further performed.

3. 5. Antioxidant Activities of MBHA and Metal Complexes

These compounds (**3**-**8**) were tested to determine their efficiency for scavenging the DPPH radicals using ascorbic acid as standard, which has a known free radical scavenging activity. The potential of MBHA and metal complexes as antioxidants has been plotted in (Fig. 5 and Fig. 6). The alcoholic MBHA and ester containing compounds are highly active against antioxidant exhibition.[28,48] The antioxidant potential of the MBHA and its transition metal complexes along with the standard (ascorbic acid) is documented in Table 4.

The results have indicated that ascorbic acid has exhibited the highest antioxidant activity at high concentration. When the highest antioxidant exhibition percent among synthesized metal moieties was compared with

Table 4. Antioxidant activity of MBHA (compound **3**) and its formed metal complexes (compound **4**-**8**)

S. No.	Concentration (mM)	Ascorbic Acid (%)	Ligand/Complexes	Antioxidant Activity (%)
1	1.00	20	**L1**	56.7
2	2.00	39.4	**CrL1**	9.7
3	3.00	58.1	**CoL1**	17.1
4	4.00	76	**NiL1**	10.8
5	5.00	92.7	**MnL1**	19.7
6	6.00	96.8	**CuL1**	18.7

DPPH scavenging effect (%) = Ac – As/Ac × 10, Ac = Absorbance of Control

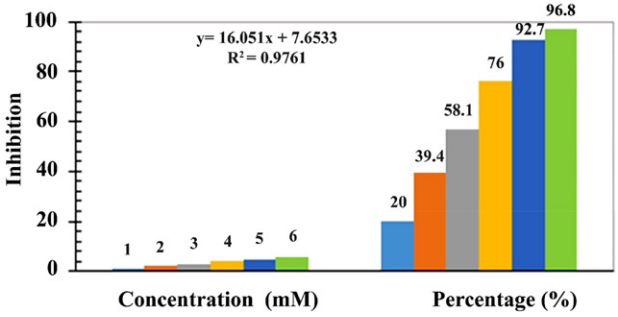

Fig. 5. Graphical representation of Antioxidant Activities of the Standard (**Ascorbic Acid**)

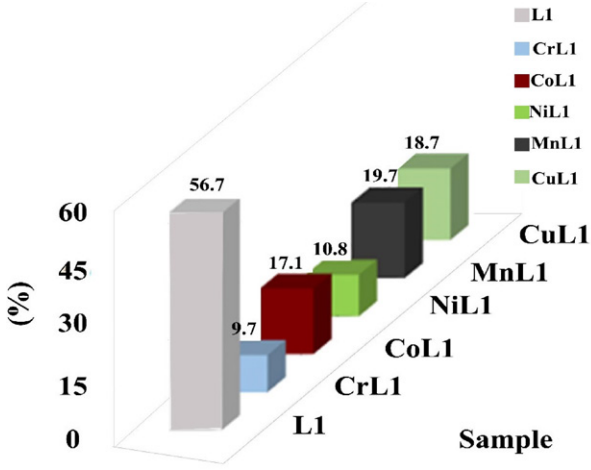

Fig. 6. Graphical representation of Antioxidant Activities of MBHA (L1) and compounds **4**-**8**

MBHA, it was observed that MnL1 (compound **7**) has the highest (19.7%) antioxidant activity. Additionally, the copper complex with MBHA has shown almost the same inhibition. However, L1 (MBHA) has comparatively maximum antioxidant activity. It is interesting to note that all these novel compounds (MBHA, $[M(L1)_2(H_2O)_4]^{+3}$ and $[M(L1)_2(H_2O)_2]^{+2}$) possess positive inhibition (Fig. 6).

3. 6. Antibacterial Assay

The antibacterial activity of these compounds was screened by using agar disc diffusion method against four

Table 5. Antibacterial activities of the MBHA and the complexes (compound **4**-**8**)

S. No	Ligand/ Complexes	*S.aureus* (%)	*E.coli* (%)	*B.pumilis* (%)	*S.typhi* (%)
1	**L1**	71.4	62.5	80.3	45.8
2	**CrL1**	A	A	40.7	A
3	**CoL1**	95.21	99.1	81.4	50.0
4	**NiL1**	44.6	45.8	40	50.0
5	**MnL1**	47.6	A	46.2	A
6	**CuL1**	52.3	A	44.4	48.0

Antimicrobial activity, expressed as inhibition zone diameter in millimeters (mm), of synthesized compounds against pathological strains based on agar well diffusion assays at 1 mg mL^{-1}. The experiment was carried out in triplicate and the average zone of inhibition was calculated.
A = Non active inhibition zone

bacterial strains (*Staphylococcus aureus, Escherichia coli, Bacillus pumilis, Salmonella typhi*) while Gentamycin is used as standard (Table 5).

The efficiency of compounds was categorized into three classes such as sensitive, transitional and resistant. The reported analysis is consistent with our findings that if a compound is found to be sensitive, it could be a valuable medication against bacterial disease. Though, non-active compounds are found to be as least resistant.[26,49,50] In contrast to the ligand an enhanced antibacterial potential was observed in metal complexes. Consequently, opening new ways in the fight against antibiotic resistance. This is because of coordination (ligand to metal) which could be best explained on the basis of chelation theory.[16,51] The comparison of antibacterial activity, shown in Fig. 7 confirms that metal complex of cobalt (compound **5**) was highly active than its corresponding MBHA ligand against all bacterial strains. It is evident from the results that all metal complexes and MBHA are significantly active against *B.pumilis,* however, chromium (compound **4**) complex is completely resistive against the remaining bacterial strains (*S.aureus, E.coli, S.typhi*). It is interesting to note that compound **7** (manganese complex) is found non-reactive against two bacterial strains (*E.coli and S. typhi*), while compound **8** (copper complex) is resistant against *E.coli* only. Thus, all remaining complexes indicate extremely positive activity against the bacterial strains.

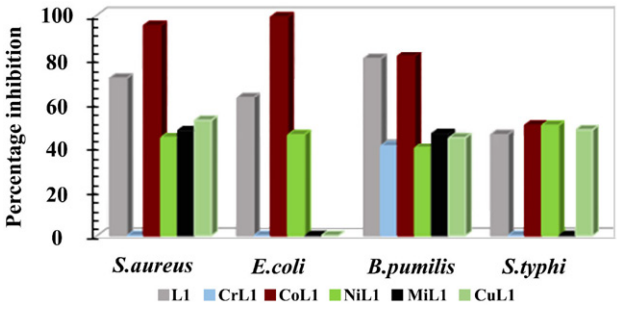

Fig. 7. A comparative histograms inhibition zone Antibacterial Assay of MBHA and compound **4-8**, S.typhi, E.coli are two Gram-negative bacteria and B.subtilis, S.aureus are two Gram- positive bacteria

4. Conclusions

An aromatic MBHA Methyl 2-((4-chlorophenyl) (hydroxy)methyle) acrylate (compound **3**) was prepared successfully by a well-known MBH reaction scheme and used further in synthesis of metal complexes by transition metal salts (Cr^{+3}, Co^{+3}, Ni^{+2}, Mn^{+2},Cu^{+2}). Through modified aforementioned scheme synthesis of five novel compounds is being reported (**4-8**). The ligand MBHA (L1) and its corresponding complexes were characterized by carrying out their physical, analytical, spectral and computational analysis. The IR spectrum of the synthesized ligand is optimized by using DFT B3LYP method and 6-311++ G (d,p) basis set. Whereas, five metal complexes were generated computationally by the Hartree Fock (HF) B3LYP method in conjunction with the 3-21G(d,p) basis set and we found good agreement with their observed FT-IR spectrum. These investigations have collectively suggested the molecular and structural formula. It has been found that MBHA (L1) coordinated with all the central metal ion in stoichiometric of 2:1 ligand to metal ratio. The well-defined crystalline homogeneous nature of all metal complexes was observed and confirmed through XRD powder diffraction analysis. Moreover, different crystal structures were found for each metal complex. Such as, compound **4** is orthorhombic, compound **6** is hexagonal, and compound **8** is monoclinic while compounds **5** and **7** both lie in cubic crystal class. For antibacterial assay, four pathogenic strains (*S. aureus, E. coli, B. pumilis, P. mirabilis, and S.typhi*) were examined and compared with standard antibiotic, Gentamycin. It was inferred that Cobalt complexes displayed uppermost antibacterial potential compared to MBHA (L1). Whereas, Nickle based complex showed good inhibition against all four bacterial strains. Chromium based complexes were found active against *B.pumilis* only. Both Manganese and Copper based complexes were seen inactive against *E. coli*. Manganese complex inhibition potential against *S.typhi* indicated non-active, conversely, again showed good inhibition zone against the remaining bacterial strains. Furthermore, the DPPH radical scavenging assay (antioxidant) of compounds **3-8** demonstrated the positive inhibition with context to the standard (ascorbic acid). This study can be expanded further by synthesizing some other novel MBHA ligands and their metal complexes, in order to identify the most suitable medication against infectious diseases.

Acknoledgement

The authors are thankful to University of Karachi for providing such an appreciative infrastructure and environment. We are highly gratified to PCSIR laboratories Complex-Karachi, Pakistan and NED University of Engineering and Technology for their support in bioactivity studies and XRD analysis opportunity**.**

Conflict of interest

All authors declare that they have no conflict of interest.

5. References

1. F. Collet, R. H. Dodd, P. Dauban, *Chem. Commun.* **2009**, Vol. *20* (34), pp. 5061–5074.
DOI:10.1039/b905820f
2. E. C. Tavares, M. M. M. Rubinger, E. V. Filho, M. R. L. Ol-

iveira, D. Piló-Veloso, J. Ellena, S. Guilardi, R. A. C. Souza, L. Zambolim, *J. Mol. Struct.* **2016**, Vol. *1106*, pp. 130–140. **DOI:**10.1016/j.molstruc.2015.10.097
3. R. O. M. A. de Souza, V. L. P. Pereira, M. F. Muzitano, C. A. B. Falcão, B. Rossi-Bergmann, E. B. A. Filho, M. L. A. A. Vasconcellos, *Eur. J. Med. Chem.* **2007**, Vol. *42* (1), pp. 99–102. **DOI:**10.1016/j.ejmech.2006.07.013
4. J. Du, Y. Ma, F. Meng, R. Zhang, R. Wang, H. Shi, Q. Wang, Y. Fan, H. Huang, J. Cui, et al., **2019**, pp. 9–12. **DOI:**10.1021/acs.orglett.8b03709
5. T. Narendar Reddy, V. Jayathirtha Rao, *Tetrahedron Lett.* **2018**, Vol. *59* (30), pp. 2859–2875. **DOI:**10.1016/j.tetlet.2018.06.023
6. M. Tsednee, Y. C. Huang, Y. R. Chen, K. C. Yeh, *Sci. Rep.* **2016**, Vol. *6* (May), pp. 1–13. **DOI:**10.1038/srep26785
7. V. Carrasco-Sanchez, M. J. Simirgiotis, L. S. Santos, *Molecules*. **2009**, Vol. *14* (10), pp. 3989–4021. **DOI:**10.3390/molecules14103989
8. G. W. Amarante, M. Benassi, R. N. Pascoal, M. N. Eberlin, F. Coelho, *Tetrahedron*. **2010**, Vol. *66* (24), pp. 4370–4376. **DOI:**10.1016/j.tet.2010.04.018
9. C. G. L. Junior, P. A. C. De Assis, F. P. L. Silva, S. C. O. Sousa, N. G. De Andrade, T. P. Barbosa, P. L. N. Nerís, L. V. G. Segundo, Í. C. Anjos, G. A. U. Carvalho, et al., *Bioorg. Chem.* **2010**, Vol. *38* (6), pp. 279–284. **DOI:**10.1016/j.bioorg.2010.08.002
10. R. V. Pirovani, B. R. V. Ferreira, F. Coelho, *Synlett*. **2009**, (14), pp. 2333–2337. **DOI:**10.1055/s-0029-1217725
11. S. Rehman, M. Ikram, F. Subhan, M. Sinnokrot, W. Khan, *Open Chem.* **2019**, Vol. *17* (1), pp. 936–942. **DOI:**10.1515/chem-2019-0108
12. D. C. Crans, J. J. Smee, E. Gaidamauskas, L. Yang, *Chem. Rev.* **2004**, Vol. *104* (2), pp. 849–902. **DOI:**10.1021/cr020607t
13. P. C. Bruijnincx, P. J. Sadler, *Curr. Opin. Chem. Biol.* **2008**, Vol. *12* (2), pp. 197–206. **DOI:**10.1016/j.cbpa.2007.11.013
14. J. Martí-Rujas, *Dalt. Trans.* **2020**, Vol. *49* (40), pp. 13897–13916. **DOI:**10.1039/D0DT02802A
15. S. Y. Liu, I. D. Hills, G. C. Fu, *Organometallics*. **2002**, Vol. *21* (21), pp. 4323–4325. **DOI:**10.1021/om020533b
16. V. B. M. Brito, G. F. Santos, T. D. S. Silva, J. L. C. Souza, G. C. G. Militão, F. T. Martins, F. P. L. Silva, B. G. Oliveira, E. C. C. Araújo, M. L. A. A. Vasconcellos, et al., *Mol. Divers.* **2020**, Vol. *24* (1), pp. 265–281. **DOI:**10.1007/s11030-019-09950-7
17. J. da Câmara Rocha, K. A. da Franca Rodrigues, P. L. do Nascimento Néris, L. V. da Silva, F. S. Almeida, V. S. Lima, R. F. Peixoto, J. da Câmara Rocha, F. de L. A. A. de Azevedo, R. C. Veras, et al., *Parasitol. Res.* **2019**, Vol. *118* (10), pp. 3067–3076. **DOI:**10.1007/s00436-019-06403-w
18. F. Coelho, W. P. Almeida, D. Veronese, C. R. Mateus, E. C. Silva Lopes, R. C. Rossi, G. P. C. Silveira, C. H. Pavam, *Tetrahedron*. **2002**, Vol. *58* (37), pp. 7437–7447. **DOI:**10.1016/S0040-4020(02)00822-0
19. M. Saikia, J. C. Sarma, *Can. J. Chem.* **2010**, Vol. *88* (12), pp. 1271–1276. **DOI:**10.1139/V10-133
20. H. Y. Qian, *Acta Chim. Slov.* **2019**, Vol. *66* (4), pp. 995–1001. **DOI:**10.17344/acsi.2019.5247
21. R. Gaussian, G. Trucks, H. Schlegel, G. Scuseria, M. Robb, J. Cheeseman, G. Scalmani, V. Barone, B. Mennucci, G. Petersson, et al., *Gaussian, Inc., Wallingford CT*. **2004**.
22. H. Ahmed, A. Hashim, H. M. Abduljalil, *Egypt. J. Chem.* **2019**, Vol. *62* (4), pp. 1167–1176. **DOI:**10.21608/ejchem.2019.6241.1522
23. A. D. Becke, *J. Chem. Phys.* **1992**, Vol. *96* (3), pp. 2155–2160. **DOI:**10.1063/1.462066
24. T. Lecklider, *EE Eval. Eng.* **2011**, Vol. *50* (11), pp. 36–39.
25. L. S. Kassel, *J. Chem. Phys.* **1936**, Vol. *4* (4), pp. 276–282. **DOI:**10.1063/1.1749835
26. S. Kirbag, F. Zengin, S. Fac, F. Processing, *Antimicrob. Act. Some Euphorbia Species*. **2013**, Vol. *10* (12), pp. 305–309. **DOI:**10.4314/ajtcam.v10i5.13
27. V. Alfredo Rodriguez, V. Alfredo, **2018**.
28. H. Elleuch, W. Mihoubi, M. Mihoubi, E. Ketata, A. Gargouri, F. Rezgui, *Bioorg. Chem.* **2018**, Vol. *78*, pp. 24–28. **DOI:**10.1016/j.bioorg.2018.03.004
29. A. L. Dawidowicz, D. Wianowska, M. Olszowy, *Food Chem.* **2012**, Vol. *131* (3), pp. 1037–1043. **DOI:**10.1016/j.foodchem.2011.09.067
30. I. Gülçin, *Arch. Toxicol.* **2012**, Vol. *86* (3), pp. 345–391. **DOI:**10.1007/s00204-011-0774-2
31. J. Mack, M. Shumba, *Green Chem.* **2007**, Vol. *9* (4), pp. 328–33. **DOI:**10.1039/B612983H
32. L. Wang, J. N. Tan, M. Ahmar, Y. Queneau, *Comptes Rendus Chim.* **2019**, Vol. *22* (9–10), pp. 615–620. **DOI:**10.1016/j.crci.2019.09.002
33. D. K. Jangid, **2020**, pp. 1–17. **DOI:**10.2174/2213346107666191227101538
34. K. Rad-moghadam, L. Youseftabar-miri, **2011**, Vol. *2011* (xi), pp. 43–50. **DOI:**10.3998/ark.5550190.0012.b04
35. M. Tsednee, Y.-C. Huang, Y.-R. Chen, K.-C. Yeh, *Sci. Rep.* **2016**, Vol. *6* (1), pp. 26785. **DOI:**10.1038/srep26785
36. E. B. A. Filho, I. A. Moraes, K. C. Weber, G. B. Rocha, M. L. A. A. Vasconcellos, *J. Mol. Struct.* **2012**, Vol. *1022*, pp. 72–80. **DOI:**10.1016/j.molstruc.2012.04.051
37. P. Marinova, M. Marinov, M. Kazakova, Y. Feodorova, A. Slavchev, D. Blazheva, D. Georgiev, P. Penchev, V. Sarafian, N. Stoyanov, *Acta Chim. Slov.* **2016**, Vol. *63* (1), pp. 26–32. **DOI:**10.17344/acsi.2015.1591
38. A. Srinivas, *Acta Chim. Slov.* **2016**, Vol. *63* (1), pp. 173–179. **DOI:**10.17344/acsi.2015.2124
39. B. Kavitha, M. Sravanthi, P. Saritha Reddy, *J. Mol. Struct.* **2019**, Vol. *1185*, pp. 153–167. **DOI:**10.1016/j.molstruc.2019.02.093
40. B. Kosar, C. Albayrak, *Spectrochim. Acta - Part A Mol. Biomol. Spectrosc.* **2011**, Vol. *78* (1), pp. 160–167. **DOI:**10.1016/j.saa.2010.09.016
41. N. Sundaraganesan, S. Kalaichelvan, C. Meganathan, B. D. Joshua, J. Cornard, *Spectrochim. Acta - Part A Mol. Biomol. Spectrosc.* **2008**, Vol. *71* (3), pp. 898–906. **DOI:**10.1016/j.saa.2008.02.016
42. Z. Yekke-Ghasemi, M. Ramezani, J. T. Mague, R. Takjoo, *New J. Chem.* **2020**, Vol. *44* (21), pp. 8878–8889. **DOI:**10.1039/D0NJ01187H
43. D. A. Köse, H. Necefoğlu, *J. Therm. Anal. Calorim.* **2008**, Vol.

93 (2), pp. 509–514. **DOI:**10.1007/s10973-007-8712-5
44. I. Kostova, I. Manolov, I. Nicolova, S. Konstantinov, M. Karaivanova, *Eur. J. Med. Chem.* **2001**, Vol. *36* (4), pp. 339–347. **DOI:**10.1016/S0223-5234(01)01221-1
45. T. Aiyelabola, E. Akinkunmi, I. Ojo, E. Obuotor, C. Adebajo, D. Isabirye, *Bioinorg. Chem. Appl.* **2017**, Vol. *2017*. **DOI:**10.1155/2017/2956145
46. M. A. Asraf, M. M. Rahman, D. C. Kabiraz, R. H. Ansary, M. F. Hossen, M. F. Haque, C. M. Zakaria, *Asian J. Appl. Chem. Res.* **2019**, Vol. *3* (3), pp. 1–15. **DOI:**10.9734/ajacr/2019/v3i330093
47. A. Jacques, T. Auvray, R. Bevernaegie, F. Loiseau, M. Cibian, G. S. Hanan, A. Kirsch-De Mesmaeker, B. Elias, *Inorganica Chim. Acta*. **2018**, Vol. *471* (Iii), pp. 8–16. **DOI:**10.1016/j.ica.2017.10.018
48. P. Jeslin Kanaga Inba, B. Annaraj, S. Thalamuthu, M. A. Neelakantan, *Bioinorg. Chem. Appl.* **2013**, Vol. *2013*. **DOI:**10.1155/2013/439848
49. B. Posssato, L. F. Dalmolin, L. M. Pereira, J. Q. Alves, R. T. C. Silva, R. V. Gelamo, A. P. Yatsuda, R. F. V. Lopez, S. de Albuquerque, N. B. Leite, et al., *Eur. J. Pharm. Sci.* **2021**, Vol. *162* (April). **DOI:**10.1016/j.ejps.2021.105834
50. K. G. Harmon, J. R. Clugston, K. Dec, B. Hainline, S. Herring, S. F. Kane, A. P. Kontos, J. J. Leddy, M. McCrea, S. K. Poddar, et al., *Br. J. Sports Med.* **2019**, Vol. *53* (4), pp. 213–225. **DOI:**10.1136/bjsports-2018-100338
51. M. I. Khan, A. Khan, I. Hussain, M. A. Khan, S. Gul, M. Iqbal, Inayat-Ur-Rahman, F. Khuda, *Inorg. Chem. Commun.* **2013**, Vol. *35* (June), pp. 104–109. **DOI:**10.1016/j.inoche.2013.06.014

Povzetek

Naslovni ligand smo sintetizirali in očistili s kolonsko kromatografijo, pri čemer smo upoštevali pomen in različna področja uporabe sintetičnih Morita-Baylis-Hillmanovih aduktov (MBHA). Pod bazičnimi pogoji smo pripravili Cr^{+3}, Mn^{+2}, Co^{+3}, Ni^{+2} in Cu^{+2} komplekse s sintetiziranim ligandom, ga karakterizirali s spektroskopskimi metodami in preverili IR spekter z izračunanim z DFT B3LYP metodo, z 6-311++ G (d,p) naborom osnov in Hartree Fock (HF) B3LYP metodo z 3-21G(d,p) naborom osnov. Dobljene kristale smo dodatno karakterizirali z rentgensko praškovno difrakcijo. Preučevali smo tudi antibakterijske in antioksidativne lastnosti MBHA in njegovih kompleksov. Vse navedene spojine so aktivni antioksidanti. Antibakterijske študije, opravljene na *S. aureus, E. coli, B. pumilis* in *S. typhi* so pokazale odlično delovanje kobaltovega kompleksa. Tovrstne spojine imajo potencial za razvoj novih, cenejših in učinkovitih zdravil za bakterijska obolenja. Raziskava predstavlja prvi primer uporabe MBHA za tvorbo kovinskih kompleksov.